Title

Multiplexed efficient on-chip sample preparation and sensitive amplification-free detection of Ebola virus

Permalink

https://escholarship.org/uc/item/2g0589zt

Authors

Du, K
Cai, H
Park, M
et al.

Publication Date

2017-05-01

DOI

10.1016/j.bios.2016.12.071

Peer reviewed

Multiplexed Efficient On-Chip Sample Preparation and Sensitive Amplification-Free Detection of Ebola Virus

K. Du[1], **H. Cai**[2], **M. Park**[1], **T. A. Wall**[3], **M. A. Stott**[3], **K. J. Alfson**[4], **A. Griffiths**[4], **R. Carrion**[4], **J. L. Patterson**[4], **A. R. Hawkins**[3], **H. Schmidt**[2], and **R. A. Mathies**[1]

[1]Department of Chemistry, University of California at Berkeley, Berkeley, CA 94720 USA

[2]School of Engineering, University of California Santa Cruz, 1156 High Street, Santa Cruz, CA 95064 USA

[3]ECEn Department, 459 Clyde Building, Brigham Young University, Provo, UT 84602 USA

[4]Department of Virology and Immunology, Texas Biomedical Research Institute, 7620 NW Loop 410, San Antonio, TX 78227 USA

Abstract

An automated microfluidic sample preparation multiplexer (SPM) has been developed and evaluated for Ebola virus detection. Metered air bubbles controlled by microvalves are used to improve bead-solution mixing thereby enhancing the hybridization of the target Ebola virus RNA with capture probes bound to the beads. The method uses thermally stable 4-formyl benzamide functionalized (4FB) magnetic beads rather than streptavidin coated beads with a high density of capture probes to improve the target capture efficiency. Exploiting an on-chip concentration protocol in the SPM and the single molecule detection capability of the antiresonant reflecting optical waveguide (ARROW) biosensor chip, a detection limit of 0.021 pfu/mL for clinical samples is achieved without target amplification. This RNA target capture efficiency is two orders of magnitude higher than previous results using streptavidin beads and the limit of detection (LOD) improves 10X. The wide dynamic range of this technique covers the whole clinically applicable concentration range. In addition, the current sample preparation time is ~1 hour which is eight times faster than previous work. This multiplexed, miniaturized sample preparation microdevice establishes a key technology that intended to develop next generation point-of-care (POC) detection system.

Introduction

Ebola is one of several known hemorrhagic fever viruses that causes an acute and serious illness in humans and other mammals. It is highly contagious and without urgent treatment leads to damage of blood vessels, organ dysfunction, and death. The recent outbreak of Ebola began in 2013 in West Africa and spread to nearly 10 countries and resulted in significant loss of life (Nouvellet et al. 2015). Since an Ebola vaccine and antiviral therapy are still not available, a rapid and simple point-of-care (POC) diagnostic test would help to control its spread by interrupting the transmission cycle. Although polymerase chain reaction (PCR) (Muyzer et al. 1993) and enzyme linked immunoassays (ELISA) (Engvall and Perlmann 1971) are now considered the gold standard for pathogen detection, they require bulky equipment, specialized laboratories, carefully curated and refrigerated reagents, and well-trained personnel which makes them problematic for routine use in low resource locations. The transportation of samples to specialized laboratories can also delay testing which increases the chances of viral transmission. Amplification-free nucleic acid detection, on the other hand, can provide a rapid and simple diagnosis test at POC which does not require specialized training and facilities. Rapid detection at local clinics would help to interrupt virus transmission by identifying positive case and unambiguously excluding the unaffected.

A number of amplification-free techniques such as plasmonic sensing (Jackman et al. 2015; Stockman 2015), electrochemical detection (Gau et al. 2005; Henihan et al. 2016), and advanced microscopy (Klamp et al. 2013; Tao et al. 2015) have been introduced to achieve sensitive detection of nucleic acid targets diagnostic of pathogens. Plasmonic sensing, relying on the spectral shift of plasmonic resonances, requires complicated fabrication techniques of noble metal nanostructures, which makes it non-ideal for low-cost and disposable devices. Electrochemical detection does not require expensive and slow patterning processes. However, the detection sensitivity is poor without target amplification. Confocal or wide-field microscopes are very sensitive but microscopes are bulky and difficult to operate at POC and require expert image interpretation. Our own work developed a viral detection technique based on an antiresonant reflecting optical waveguide (ARROW) which creates femtoliter excitation volumes on a chip to effectively excite and detect individual labeled target DNA or RNA molecules (Ozcelik et al. 2015; Schmidt and Hawkins 2011). The fluorescent burst signal is recorded as reagents flow through the liquid-core. This optofluidic platform has demonstrated single molecule detection capability in the laboratory but the extension of this powerful technique for routine use in the field requires coupling with automated sample preparation (Cai et al. 2015; Liu et al. 2015; Schmidt and Hawkins 2016).

Microfluidics with its advantages of low volume consumption, flexibility, disposability, and low costs, is a powerful tool for addressing POC sample preparation challenges (Elvira et al.

2013; Sackmann et al. 2014; Tan et al. 2015; Thompson et al. 2015). Because the channel and reactor sizes are at the micrometer scale, multiple assays can be performed in a small area in parallel. However, due to the low specific Reynolds number of liquids in microfluidic channels and reservoirs, the mixing of regents is limited due to the absence of turbulent or convective mixing (Lee et al. 2011; Wang et al. 2014). Equilibration of different phases such as solid beads and liquid is even more difficult in microfluidic devices. Several techniques have been introduced to enhance mixing in microfluidic systems, but most require additional complex devices and processes such as high DC voltage (Fang et al. 2015), microelectromechanical systems (Frommelt et al. 2008; Suzuki et al. 2004) and rotors (Jackson et al. 2016; Strohmeier et al. 2015). We thus sought to develop a simple and efficient technique to improve microfluidic mixing that does not include complex fabrication or devices.

Recently, the hybrid optofluidic integration of microfluidic sample preparation and optical sensing has come to the fore (Parks et al. 2014; Testa et al. 2014). This has led to the successful demonstration of amplification-free detection of Ebola nucleic acids on an ARROW chip, following partial sample preparation on a microfluidic chip (Cai et al. 2015). While a low limit of detection and a large dynamic range were demonstrated, the performance of the system did not reach the level required for a point-of-care device. This reduced performance was primarily due to limitations in the sample mixing and handling capabilities of the previous chip design. Here, we present a novel sample preparation multiplexer (SPM) which dramatically improves the optofluidic system in terms of target extraction efficiency, speed, and throughput. The key unique feature of the SPM is the use of metered air bubbles to stir up the magnetic beads carrying the capture probes to effect rapid and efficient target capture. Target capture, wash, and release are all carried out automatically on chip without manual intervention. This powerful microfluidic sample preparation technique improves the limit of detection by an order of magnitude and reaches the levels required for presymptomatic detection of infection (Towner et al. 2004).

Materials and Methods

Microfluidic chip fabrication

The fabrication method for the automated microfluidic sample preparation multiplexer (see designs in Figure 1a and b) with lifting-gate microvalves has been reported previously (Kim et al. 2013; Kim et al. 2012; Kim et al. 2016). The fabrication and bonding of the pneumatic layer is simple and does not require complex microfabrication process or equipment. A Graphtec Craft Robo Pro CE5000-40 Cutting Plotter (Graphtec America. Inc.) was used to cut fluidic layer patterns on 100 μm thick vinyl adhesives (3M Scotchcal 220, Gerber Scientific Products, Inc.). The sticker pattern was then transferred to a petri dish and covered with a 300 μm polydimethylsiloxane (PDMS) membrane by spin coating. To form the pneumatic layer, SU-8 microstructures (thickness ~150 μm) were exposed and developed on a silicon wafer by using photolithography. PDMS was poured on the microstructures and cured to a final thickness of ~5 mm. After peeling off the pneumatic layer from the SU-8 master, holes for pneumatic control were punched and the pneumatic layer was bonded to the fluidic layer by UV-Ozone treatment and heat. After bonding was completed, the fused

layers were peeled off the petri dish and transferred to a glass substrate. The diameter of the microvalves is ~2 mm (pumping capacity ~250 nL per stroke) and the diameter of the incubation reservoirs is ~4 mm (capacity of ~50 μL).

Sample preparation

Nucleic acid target—Synthetic nucleic acid targets (for sequence see Table S1) were purchased from Integrated DNA Technologies, Inc. (IDT) and was designed to complement the Zaire Ebola Virus (GeneBank ID AY354458.1, nt. 6832–6931). For clinical samples, Zaire Ebola Virus RNA (GeneBank ID AY354458.1) was used as positive control. Sudan Ebola virus strain Boniface RNA (Genebank ID FJ968794.1) was used as negative control. The preparation of clinical samples was carried out in the Biosafety Level 4 Laboratory at Texas Biomedical Research Institute. Briefly, a stock solution of virus was first used to infect Vero E6 cells at 90% confluence. After several days of infection, the supernatant was removed, clarified, and stored in an ultralow temperature freezer. A modified version of the loop drop method was used to determine the concentration of virus particles (Griffiths et al. 1998; Watson et al. 1963). Then, RNA was extracted from the supernatant using Trizol LS reagents (Thermo Fisher Scientific).

4FB pull-down beads—5′ Amino Modifier C6 oligonucleotides with a probe length from 25 to 70 bp were purchased from IDT. The sequences of the capture probes are given in Table S1. The probe was dissolved in 1X modification buffer (100 mM phosphate, 150 mM NaCl, pH 8.0) at a concentration of 100 μM. Seven hundred picomoles of oligonucleotide were transferred to a new Eppendorf tube and 35 μL of dimethylformamide (DMF) was added to the oligonucleotide solution. S-HyNic (1 mg, Solulink, Inc.) was dissolved in 100 μL DMF. Then, 4 μL of the S-HyNic solution was added to the oligonucleotide solution. After two hours, the HyNic modified oligonucleotide was desalted by using Zeba desalting columns (Thermo Fisher Scientific) with 1X conjugation buffer (100 mM phosphate, 150 mM NaCl, pH 6.0). A hundred microliters of 4FB beads (Solulink, Inc.) were taken from the stock solution and washed by four aliquots of 1X conjugation buffer. HyNic modified oligonucleotide was added to 100 μL 4FB beads. The pull-down beads were mixed by using a rotary mixer at room temperature for two hours. After that, the pull-down beads were washed by 1X conjugation buffer (100 mM phosphate, 150 mM NaCl, pH 6.0) four times at room temperature to remove unbound oligonucleotide and then washed with T50 (10 mM Tris, 50 mM NaCl, pH 8.0) four times followed by re-suspension in 100 μL T50 buffer. The final concentration of the 4FB beads is 10 mg/mL.

Streptavidin pull-down beads—The 5′ Biotin-TEG modified capture oligonucleotide was purchased from Integrated DNA Technologies, Inc. (IDT). One milligram of Dynabeads® MyOne™ Streptavidin T1 beads were washed with four aliquots of T50 buffer. Seven hundred picomoles of capture oligonucleotide were added to the magnetic bead solution followed by incubation at room temperature using a rotary mixer for two hours. The unbound oligonucleotide was removed by four T50 washes followed by re-suspension in 100 μL T50 buffer. For the washing experiments, 4FB beads were heated to 50 °C for 5 minutes in a water bath (~5 mL) and washed with T50 four times (2 cycles). They were then heated to 80 °C for 2 minutes and washed with T50 four times (5 cycles). The first supernatant (100

µL) from every washing cycle was collected, stained by SYBR® Gold dye, and measured using the JASCO FP-750 (JASCO) to determine how much capture oligonucleotide was washed off.

On-chip solid-phase extraction

One microliter of the 4FB bead suspension (10 mg/mL) was added to each incubation reservoir and nucleic acid samples were pumped into the incubation reservoirs through the microvalve system. Metered air bubbles (~1.5 µL/s) were then introduced to each incubation reservoir for 30 seconds to effect mixing. A TEC heater (Thorlabs, Inc.) was used to heat the incubation reservoirs to ~40 °C. Thirty seconds of air bubble mixing was performed every 10 minutes to keep the beads suspended. The closing pressure was set at 40 kPa and the actuation time was 150 ms. After incubation, a magnet was placed under each incubation reservoir to pull down the beads so that the supernatant could be evacuated through the microvalves. The magnet was removed and then T50 buffer was pumped from the inlet into the incubation reservoirs to fill the incubation reservoirs (~45 µL) followed by re-suspension of the beads by 30 seconds of air bubble mixing. Again, magnets were used to pull down the beads and the buffer solution was removed. The washing cycle was repeated two times to reduce non-specific binding and unbound targets. Then, T50 buffer was pumped into the incubation reservoirs and the reagents were heated to ~80 °C to release captured nucleic acid targets from the beads. Finally, the beads were collected by magnets and the supernatant was removed for the fluorescence measurements. A glass slide covers the incubation reservoirs during processing to avoid contaminations from/to the environment. After use, the PDMS layers were peeled off from the glass substrate, cleaned with isopropyl alcohol and nuclease-free water, and then stored in biosafety cabinet for later use. For work dealing with infectious reagents, the microfluidic chip should not be re-used.

Fluorescence quantitation

The capture efficiency of each synthetic nucleic acid target was measured by using a custom fluorometer consisting of a compact laser module (443 nm) and a fiber spectrometer (Figure S1a). The power of the excitation light was reduced to ~70 mW to avoid sample damage and focused onto the sample with a ~1 mm diameter spot size. Fluorescence was collected with a lens-adapted optical fiber connected to a USB 2000+ spectrometer (Ocean Optics Inc.), and all data were analyzed by using Spectra Suite Pro software (Ocean Optics Inc.). In a typical experiment, 10 µL of DNA sample diluted with 280 µL T50 buffer and 10 µL SYBR® Gold (1X) was added to the diluted solution for detection. The fluorescence peak intensities at 537 nm were used to evaluate the capture efficiencies (Figure S1b) and they were linearly dependent on nucleic acid concentration (Figure S1c).

Single Molecule Fluorescence Detection

Antiresonant reflecting optical waveguide (ARROW) chip fabrication—The
optofluidic chip was fabricated on a four inch silicon wafer on which a sequence of dielectric layers for optical guiding was deposited(Cai et al. 2015). These cladding layers consisted of Ta_2O_5 and SiO_2 (refractive index: 1.07 and 1.46) having thicknesses in nanometers starting from the substrate of 265/102/265/102/265/102, where the material

sequence is $SiO_2/Ta_2O_5/SiO_2/Ta_2O_5/SiO_2/Ta_2O_5$. SU8 photoresist (SU8–10, MicroChem) was spun on the wafer, patterned and developed to define the hollow waveguide channel with a rectangular cross section of 12 μm wide by 5 μm high. The hollow waveguide sits on a pedestal which was fabricated by dry etching in an inductively-coupled-plasma reactive ion etcher (ICP-RIE) using the SU8 and a thin nickel layer as the mask. A single SiO_2 overcoat layer of 6 μm thickness was then deposited over the SU8 by plasma-enhanced chemical vapor deposition. Three micron tall ridges were etched into the SiO_2 layer, again using the ICP-RIE, to form ridge waveguides that intersect multiple points of the hollow waveguide. Fluid inlets into the hollow channel were exposed with a buffered HF wet etch through the top SiO_2 layer and the SU8 was then removed with a H_2SO_4:H_2O_2 solution to form the hollow core (Ozcelik et al. 2015; Ozcelik et al. 2016). The schematic drawing and scanning electron microscope (SEM) image of the hollow core of the ARROW chip is shown in Figure S3. After rinsing the wafer in deionized water, it was cleaved into individual chips of approximately 10×12 mm^2. The ARROW chip was annealed at ~300 °C for 8 hours in an air atmosphere to improve the chip performance by reducing water absorption in the porous oxide (Parks et al. 2014).

Single molecule detection—For the proof of principle experiments, we mixed the prepared RNA samples with 0.1X SYBR® Gold for ~20 minutes and put the mixture into the liquid-core ARROW channel through one of the reservoirs connecting the inlet of the channel as schematically shown in Figure 1 (c). Negative pressure was applied to the other reservoir to enable constant flow inside the liquid-core ARROW channel. For fluorescence detection, an Ar-ion laser (488 nm) was coupled to the solid-core ARROW from a single mode fiber to excite the fluorescent RNA at the solid-core/liquid-core waveguide intersection. The generated fluorescence signal propagated orthogonally in the liquid-core ARROW channel and was guided to the chip edge where it was collected, filtered (Semrock, BLP01-532R-25), and detected by a photodiode (Perkin-Elmer, SPCM-AQR-14). Before each sample measurement, a control measurement using only SYBR® Gold dye at a concentration of 0.1X was carried out to record the background fluorescence signal for the same amount of recording time (1 to 10 minutes) as the sample measurement. We select the highest background photon count recorded in this way as the threshold for identifying a positive target detection event. The recorded photon counts for each event are normalized to the detected throughput power from the excitation waveguide output to eliminate the effect of power fluctuation due to variance in fiber-to-chip coupling.

Results

The sample preparation multiplexer (SPM), consisting of incubation reservoirs connected to a network of microchannels and microvalves (Figure 1a), is designed to run six on-chip bead-based solid-phase DNA or RNA target extraction assays in parallel. The pneumatic layer (green) pneumatically controls the opening and closing of the microvalves driven by off-chip solenoid valves and a custom LabVIEW program. Reagents are introduced and transported in the red fluidic layer. Switching from pressure (45 kPa) to vacuum (80 kPa) at the inlets on the pneumatic layer opens the microvalves enabling automated transfer of fluids. A photograph of the device is presented in Figure 1 (b). Thin channels (120 μm wide,

100 μm deep) are employed for the pneumatic layer to avoid delamination during microvalve actuation. For the fluidic layer, four 300 μm wide, 100 μm deep channels are connected to each 4-mm diameter, 4.5-mm deep incubation reservoir to introduce reagents.

The procedure for on-chip solid-phase extraction is outlined in Figure 1 (c). (i) First nucleic acid targets are pumped into the incubation reservoirs and mixed with a suspension of magnetic microbeads conjugated with a capture probe. (ii) Air bubbles are periodically pumped through the reservoirs to enhance capture by stirring up the beads. (iii) Through this process, targets with matched sequences are captured by hybridizing to the capture probes. (iv) A magnet is used to pull down the beads leaving the mismatched sequence in the supernatant and the beads are washed at elevated temperature to remove weakly bound nonspecific sequences. (v) Captured targets are released from the magnetic beads by denaturing the double strand hybrid with heat. (vi) Finally, the released targets are stained by SYBR® Gold and detected using the ARROW chip.

The SPM is designed to enhance mixing between the target solution and the beads resulting in efficient capture. During incubation, unstirred magnetic beads settle to the bottom of the incubation reservoirs and do not equilibrate with the entire solution. To re-suspend the beads for enhanced target capture, three microvalves in series open and close sequentially to pass metered air bubbles from the inlets to the incubation reservoirs (Figure 2a). The metered bubbles induce convective mixing in the incubation reservoirs. With no mixing, most of the beads settle to the bottom in only 15 minutes (Figure 2b). However, after air bubble mixing for 30 seconds, the beads are effectively re-suspended as indicated by the uniform light brown color in the reservoir (Figure 2b).

To verify that air bubble mixing produces optimum target capture, an experiment was carried out mixing the 70-mer pull-down beads and a synthetic nucleic acid target and determining the pull-down efficiency. During incubation (40 minutes overall), various air pumping times (30 seconds/every 10 minutes, 60 seconds/every 10 minutes, 180 seconds/every 10 minutes, and 300 seconds/every 10 minutes) were applied. After incubation and release, the target samples were stained by SYBR Gold® dye and the fluorescence signal was measured vs. diluted target stock. Figure 2 (c) summarizes the target capture efficiency for different air pumping times. Thirty seconds of air bubble mixing every 10 minutes improves the target capture efficiency to 35%, which is a 1.4X improvement over no mixing. For our previous microfluidic design, one order of magnitude lower target capture efficiency was observed compared with off-chip processing (Cai et al. 2015). Our new fully automated microfluidic sample preparation device with air bubble mixing demonstrates a capture efficiency that is the same as manual off-chip preparation (~35%). The automated microfluidic sample preparation avoids the time consuming manual operation and can reliable process multiple samples. Increasing the air bubble pumping time further does not significantly improve the capture efficiency. Hence, 30 seconds of air pumping every 10 minutes is sufficient to optimize reagent mixing and achieve optimum capture.

The capture efficiency was further improved by tuning the incubation and releasing conditions. As presented in Figure 3, incubation times ranging from 10 to 60 minutes and release times ranging from 2 to 10 minutes were examined. For all the experiments, 70-mer

magnetic beads and 20 μL synthetic nucleic acid target (1 nM) were employed. During incubation, air bubbles were introduced for 30 seconds every 10 minutes to suspend the magnetic beads. Increasing the incubation time from 10 to 60 minutes (without changing the releasing time) does not significantly improve the capture efficiency: This suggests that the hybridization is complete within 10 minutes. We observed magnetic beads adsorption on the PDMS walls after 60 minutes of incubation, which explains the decrease of capture efficiency at longer times. However, the capture efficiency is very sensitive to the release time. The capture efficiency is highest for an 8 minutes release time. Because the melting temperature for the target/capture probe is ~70 °C, allowing sufficient time for uniform heating of the incubation reservoirs to 80 °C is critical for denaturation and release.

The SPM is also designed to enable an on-chip concentration step to extend the detection limit. For example, we incubated 45 μL of 100-mer synthetic nucleic acid target with 70-mer coated magnetic beads. After incubation and washing, the targets were released in 15 μL T50 solution, resulting in a threefold concentration increase (3X). The released samples were stained by SYBR® Gold and compared with the unconcentrated solution (20 μL input, 20 μL release). Various incubation times ranging from 10 to 60 minutes were explored to optimize the hybridization conditions. A release time of 10 minutes allowed complete release of the targets. As shown in Figure 4, higher fluorescence signals were detected with the 3X sample process regardless of the incubation time. For the 3X on-chip concentration protocol, the fluorescence signal is ~90% of the unprocessed solution (1 nM), which is a ~60% improvement of the capture efficiency over the 1X protocol. The 3X concentration when performed with our new chip provides a 53% capture efficiency which is essentially the same as the 56% efficiency delivered in our earlier study (Cai et al. 2015). However, for the new chip and protocol, the hybridization, concentration, and target release were all integrated in the microfluidic chip and thus require much less processing time and complexity.

Low concentration Ebola clinical samples were prepared using the SPM and detected using the ARROW chip. With the optimized conditions in hand, we determined the LOD, dynamic range, and linearity. The incubation time was 40 minutes (30 seconds air bubble mixing/10 minutes) and the releasing time was 8 minutes at 80 °C. A representative measurement is presented in Figure 5 (inset) with multiple peaks recorded with a target concentration of 0.21 pfu/mL. Due to the high specificity of the solid-phase extraction method, no peaks were detected above dye background for the negative control sample (SUDV). On the other hand, fluorescence peak counts show a linear dependence on concentration for positive EBOV samples over a total of 5 orders of magnitude.

We first consider the case of off-chip sample preparation of EBOV with the 4FB beads. The increased count rate for a given concentration in the red trace indicates that the capture efficiency is 5–10 times higher than the off-chip sample preparation using the Streptavidin beads (dark blue). We then performed an on-chip sample preparation of EBOV with the 3X concentration method using the optimized incubation and releasing conditions. The fluorescence intensity in light blue shows a linear dependence over 4 orders of magnitude down to 0.21 pfu/mL (pea green) with 3X on-chip concentration and the process time is 40 minutes. The result shows a similar capture efficiency as the off-chip case. It does not

require hundreds folds of preconcentration and several hours of process time (Cai et al. 2015). In addition, using the 4FB beads improves the capture efficiency of EBOV by 2 orders of magnitude over the on-chip experiments using Streptavidin beads (green) (Cai et al. 2015). The improved performance is due to the high density of capture probes on the 4FB beads (off-chip) and enhanced mixing with microfluidic multiplexer (on-chip).

We were able to extend the LOD using an 80X on-chip concentration approach (dashed circle in Figure 5). An incubation reservoir with a larger 100 μL capacity was used and the capture and wash processes were repeated 8 times to allow the magnetic beads (1 μL) to repetitively capture targets for detection. Finally, the targets were released in 10 μL buffer solution for ARROW chip detection providing 0.021 pfu/mL detection limit.

Discussion

Solid phase affinity techniques are frequently used for sample preparation by immobilizing capture probes on one or more surfaces of a microfluidic chip; however, the total capture surface area in these formats is often limited (Huang et al. 2015; Normann et al. 2004). Functionalized magnetic beads, one the other hand, offer a higher surface area resulting in higher capture efficiency, but one must develop an effective way to incorporate them into the chip format. Because magnetic beads rapidly settle during hybridization and form clusters, access to binding sites is reduced and it takes longer for the targets to diffuse to the capture probes. These effects reduce the efficiency of capture and increase the time required for hybridization. Furthermore, during sample preparation, the problems of bead sticking, adsorption, and loss during transportation in the microfluidic system leads to loss of beads. All these problems lead to poor target capture efficiency.

In our SPM, the capture, wash, and release processes are all carried out in the incubation reservoirs. By only transporting liquids to/from the incubation reservoirs in the microchannels, we avoid the problems of trapping and losing beads in microchannels or microvalves and microchannel obstruction. In the incubation reservoirs, metered air bubbles are used to keep the beads in suspension and thereby enhance the rate and efficiency of target capture. The air pumping volume per stroke is controlled by the size of the microvalves and the air pumping rate is controlled by the solenoid valve timing. The current microvalve size is ~0.47 μL and volumetric flow rate is set at ~1.5 μL air/s. These parameters are easily adjusted to satisfy different mixing needs. Uniform mixing of magnetic beads and nucleic acids is achieved by pumping air bubbles for 30 seconds every 10 minutes. By regulating the air flow with microvalves to produce bubbles with a diameter less than 1mm, the air pumping volume and timing is precisely controlled avoiding reagent blowout.

Although other methods such as an acoustic mixer (Frommelt et al. 2008), electrophoresis mixer (Fang et al. 2015), microfabricated conductors (Suzuki et al. 2004), motor controlled rotational magnets (Jackson et al. 2016), and an on-chip centrifuge (Strohmeier et al. 2015) have been introduced to enhance the mixing of magnetic beads and nucleic acids, they all increase the instrument size/weight, fabrication costs, power consumption, and operation complexity which is not desired for resource-limited settings. In our case, since the air

bubbles are injected through pneumatically actuated microvalves, the solenoid valves used for fluid control also conveniently produce the bubbles. In addition, since the air bubbles are pumped into the incubation reservoirs from common channels, additional layers and chambers to diffuse air bubbles for enhanced mixing are not needed (Lin et al. 2014).

Streptavidin modified beads are typically used to immobilize capture agents such as oligonucleotides (Frock et al. 2015; Thorslund et al. 2015) but they have their disadvantages. The non-covalent streptavidin-biotin bond formation is rapid and very stable at room temperature; however, streptavidin can be denatured and partial dissociated at elevated temperatures. In our case, the heating step used to release the target RNA from the probe leads to the partial dissociation of streptavidin tetramers, releasing the capture probes into the assay. As the proprietary unsymmetrical cyanine dye binds nonspecifically to both RNA and DNA, the presence of the capture probe leads to elevated background. Pre-washing the streptavidin beads at high temperature before the on-chip capture experiment reduced the capture probe release background, but it also reduced the density of capture probes on the beads and resulted in a lower capture efficiency. To address this problem, 4-formyl benzamine functionalized (4FB) and Hynic linker was used. The covalent bond between the bead and the DNA probe was found to be more stable at the high temperature used to release the RNA target. Also, only a few wash cycles at mild temperature are needed to remove the non-specific capture probe background. Because the initial surface density of capture probes are the same for streptavidin beads and 4FB beads, the density of the capture probes remaining on the magnetic beads is higher for 4FB beads than streptavidin beads: We conclude that the 4FB bead modification procedure is superior to streptavidin-biotin and enables higher capture efficiency and improved detection sensitivity.

Exploiting these advances, we developed an efficient multiplexed on-chip sample preparation and sensing technique for Ebola virus diagnosis. With the metered air bubble mixing and thermally stable pull-down beads, we improved the capture efficiency by 2 orders of magnitude compared to our previous on-chip experiments using in-valve target capture and streptavidin beads (Cai et al. 2015). The sample preparation process is automated and exhibits the same capture efficiency as manual off-chip processing. Combined with amplification-free counting of single molecules using the ARROW chip, we achieved a limit of detection of 0.21 pfu/mL using 3X on-chip concentration with only 40 minutes incubation time. Although same detection limit was reported using in-valve target capture and streptavidin beads, it requires nearly 500X preconcentration and more than 8 hours incubation time (Cai et al. 2015). In addition, using the new on-chip concentration protocol (80X), we push the detection limit to 0.021 pfu/mL which is one order of magnitude higher than previous results. This approach shows great sensitivity, specificity, and a wide dynamic range required for a practical clinical assay and has a similar sensitivity as PCR (Trombley et al. 2010).

Other amplification-free techniques such as nanoplasmonic sensing have been used to detect virus targets by measuring the changes of the permittivity of the dielectric adjacent to the metal nanostructures caused by binding (Jackman et al. 2015; Stockman 2015). This requires that the capture probe be immobilized on the metal surfaces, which limits the total capture surface area. In addition, the high sensitivity of nanoplasmonic sensing has only

been observed on uniform nanometer scale structures. It requires expensive and slow patterning techniques such as electron beam lithography (EBL) (Gordon et al. 2010) and nanoimprint lithography (NIL) (Zhu et al. 2015) which is not easy for mass production and is not desired for simple and disposable detection instruments at POC. More importantly, our technique shows much higher sensitivity and selectivity than nanoplasmonic sensing and other amplification-free techniques by orders of magnitude (Gau et al. 2005; Henihan et al. 2016; Jackman et al. 2015; Klamp et al. 2013; Stockman 2015; Tao et al. 2015).

SPM allows running multiple assays in parallel using small volume samples at the microliter scale (~60 μL for 3X and ~800 μL for 80X). When working with whole blood samples, cell lysis and RNase denaturation are required to obtain intact viral RNA (Tan and Yiap 2009). It has been shown that 80%–95% of the total viral RNA can be rapidly isolated from 200 μL of whole blood using an off-chip commercial method (ZR Whole-Blood RNA MiniPrep™), thus our sample preparation protocol is compatible with the fingerprick blood test (Anderson et al. 1999). Fingerprick blood samples are easier to obtain than needle draws, can be collected from several sites on the body, and can be done with little training. Viral RNA extraction from whole blood can also be achieved on-chip by using a cell lysis reagent (Hui et al. 2007) and filtering process (Liu et al. 2016). In our own work, whole blood filtration and nucleic acid extraction have been demonstrated by using PDMS microfluidic devices in combination with ARROW chips for multiplex optical detection of cancer biomarkers (Cai et al. 2016). All these advantages are helpful when operating in resource-limited settings. With the optimized hybridization conditions, the total sample preparation and detection time is less than 2 hours which is comparable with typical PCR analysis (Drosten et al. 2002; Towner et al. 2004). The rapid detection demonstrated here could determine the viral loads of suspected patients at POC without quarantining or housing the suspected patients in holding units for many hours or even days waiting for the PCR analysis. As the viral load of infected cases can reach 0.04 pfu/mL in the serum before the onset of symptoms, our approach with 0.021 pfu/mL sensitivity could provide crucial information for early clinical decisions by confirming or clearing suspected patients before symptoms such as nausea, cough, and bleeding are shown. Compared to non-fatal cases in which viral load does not increase significantly after posting symptoms, the viral load of fatal cases can rapidly increase to 2–50 pfu/mL at the first day of posting symptoms (Zaki et al. 1999). The wide dynamic range of our approach could provide insight into the seriousness of the infection.

We have demonstrated a key technology that will enable the next generation of Ebola hemorrhagic fever virus (HFV) and other infectious disease detection at the POC with an instrument having excellent sensitivity, specificity, and a wide dynamic range that does not require nucleic acid amplification. By decreasing the diameter of the incubation reservoirs to 2.5 mm and the width of microchannels to 300 μm, 64 assays could be performed at the same time in parallel on a 5 inch chip to increase the throughput. This improvement will help to rapidly screen multiple suspicious cases in the infected communities at low cost. As regulated air pumps, lasers and detectors, and micro heaters are small in size, it is feasible to integrate all the components in a compact unit as we have done previously in other applications (Skelley et al. 2005).

Supplementary Material

Refer to Web version on PubMed Central for supplementary material.

References

Anderson T, SU XZ, Bockarie M, Lagog M, Day K. Parasitology. 1999; 119(02):113–125. [PubMed: 10466118]

Cai H, Parks JW, Wall TA, Stott MA, Stambaugh A, Alfson K, Griffiths A, Mathies RA, Carrion R, Patterson JL, Hawkins AR, Schmidt H. Sci Rep. 2015; 5:14494. [PubMed: 26404403]

Cai H, Stott MA, Ozcelik D, Parks JW, Hawkins AR, Schmidt H. Biomicrofluidics. 2016; 10(6): 064116. [PubMed: 28058082]

Drosten C, Göttig S, Schilling S, Asper M, Panning M, Schmitz H, Günther S. J Clin Microbiol. 2002; 40(7):2323–2330. [PubMed: 12089242]

Elvira KS, I Solvas XC, Wootton RC. Nat Chem. 2013; 5(11):905–915. [PubMed: 24153367]

Engvall E, Perlmann P. Immunochemistry. 1971; 8(9):871–874. [PubMed: 5135623]

Fang F, Zhang N, Liu K, Wu ZY. Microfluid Nanofluid. 2015; 18(5–6):887–895.

Frock RL, Hu J, Meyers RM, Ho YJ, Kii E, Alt FW. Nat Biotechnol. 2015; 33(2):179–186. [PubMed: 25503383]

Frommelt T, Kostur M, Wenzel-Schäfer M, Talkner P, Hänggi P, Wixforth A. Phys Rev Lett. 2008; 100(3):034502. [PubMed: 18232985]

Gau V, Ma SC, Wang H, Tsukuda J, Kibler J, Haake DA. Methods. 2005; 37(1):73–83. [PubMed: 16213156]

Gordon R, Brolo AG, Sinton D, Kavanagh KL. Laser Photon Rev. 2010; 4(2):311–335.

Griffiths A, Renfrey S, Minson T. J Gen Virol. 1998; 79(4):807–812. [PubMed: 9568976]

Henihan G, Schulze H, Corrigan DK, Giraud G, Terry JG, Hardie A, Campbell CJ, Walton AJ, Crain J, Pethig R. Biosens Bioelectron. 2016; 81:487–494. [PubMed: 27016627]

Huang F, Zhou X, Yao D, Xiao S, Liang H. Small. 2015; 11(43):5800–5806. [PubMed: 26382921]

Hui WC, Yobas L, Samper VD, Heng CK, Liw S, Ji H, Chen Y, Cong L, Li J, Lim TM. Sensors and Actuators A: Physical. 2007; 133(2):335–339.

Jackman JA, Linardy E, Yoo D, Seo J, Ng WB, Klemme DJ, Wittenberg NJ, Oh SH, Cho NJ. Small. 2015; 12(9):1159–1166. [PubMed: 26450658]

Jackson K, Borba J, Meija M, Mills D, Haverstick D, Olson K, Aranda R, Garner G, Carrilho E, Landers J. Anal Chim Acta. 2016; 937:1–10. [PubMed: 27590539]

Kim J, Jensen EC, Stockton AM, Mathies RA. Anal Chem. 2013; 85(16):7682–7688. [PubMed: 23675832]

Kim J, Kang M, Jensen EC, Mathies RA. Anal Chem. 2012; 84(4):2067–2071. [PubMed: 22257104]

Kim J, Stockton AM, Jensen EC, Mathies RA. Lab Chip. 2016; 16(5):812–819. [PubMed: 26864083]

Klamp T, Camps M, Nieto B, Guasch F, Ranasinghe RT, Wiedemann J, Petrášek Z, Schwille P, Klenerman D, Sauer M. Sci Rep. 2013; 3:1852. [PubMed: 23677392]

Lee CY, Chang CL, Wang YN, Fu LM. Int J Mol Sci. 2011; 12(5):3263–3287. [PubMed: 21686184]

Lin YH, Wang CC, Lei KF. Biomed Microdevices. 2014; 16(2):199–207. [PubMed: 24141738]

Liu C, Liao SC, Song J, Mauk MG, Li X, Wu G, Ge D, Greenberg RM, Yang S, Bau HH. Lab Chip. 2016; 16(3):553–560. [PubMed: 26732765]

Liu S, Wall TA, Ozcelik D, Parks JW, Hawkins AR, Schmidt H. Chem Comm. 2015; 51(11):2084–2087. [PubMed: 25533516]

Muyzer G, De Waal EC, Uitterlinden AG. Appl Environ Microbiol. 1993; 59(3):695–700. [PubMed: 7683183]

Normann A, Jung C, Vallbracht A, Flehmig B. J Med Virol. 2004; 72(1):10–16. [PubMed: 14635005]

Nouvellet P, Garske T, Mills HL, Nedjati-Gilani G, Hinsley W, Blake IM, Van Kerkhove MD, Cori A, Dorigatti I, Jombart T, Riley S, Fraser C, Donnelly CA, Ferguson NM. Nature. 2015; 528(7580): 109–116.

Ozcelik D, Parks JW, Wall TA, Stott MA, Cai H, Parks JW, Hawkins AR, Schmidt H. Proc Natl Acad Sci USA. 2015; 112(42):12933–12937. [PubMed: 26438840]

Ozcelik D, Stott MA, Parks JW, Black JA, Wall TA, Hawkins AR, Schmidt H. IEEE J Sel Top Quantum Electron. 2016; 22(4):1–6.

Parks J, Olson M, Kim J, Ozcelik D, Cai H, Carrion R Jr, Patterson J, Mathies RA, Hawkins AR, Schmidt H. Biomicrofluidics. 2014; 8(5):054111. [PubMed: 25584111]

Sackmann EK, Fulton AL, Beebe DJ. Nature. 2014; 507(7491):181–189. [PubMed: 24622198]

Schmidt H, Hawkins AR. Nat Photonics. 2011; 5(10):598–604.

Schmidt H, Hawkins AR. Bioanalysis. 2016; 8(9):867–870. [PubMed: 27094821]

Skelley AM, Scherer JR, Aubrey AD, Grover WH, Ivester RH, Ehrenfreund P, Grunthaner FJ, Bada JL, Mathies RA. Proc Natl Acad Sci USA. 2005; 102(4):1041–1046. [PubMed: 15657130]

Stockman MI. Science. 2015; 348(6232):287–288. [PubMed: 25883343]

Strohmeier O, Keller M, Schwemmer F, Zehnle S, Mark D, von Stetten F, Zengerle R, Paust N. Chem Soc Rev. 2015; 44(17):6187–6229. [PubMed: 26035697]

Suzuki H, Ho CM, Kasagi N. J Microelectromech Syst. 2004; 13(5):779–790.

Tan SC, Yiap BC. BioMed Research International. 2009; 2009

Tan Y, Tang T, Xu H, Zhu C, Cunningham BT. Biosens Bioelectron. 2015; 73:32–40. [PubMed: 26043313]

Tao Y, Rotem A, Zhang H, Chang CB, Basu A, Kolawole AO, Koehler SA, Ren Y, Lin JS, Pipas JM. Lab Chip. 2015; 15(19):3934–3940. [PubMed: 26304791]

Testa G, Persichetti G, Sarro PM, Bernini R. Biomed Opt Express. 2014; 5(2):417–426. [PubMed: 24575337]

Thompson BL, Ouyang Y, Duarte GR, Carrilho E, Krauss ST, Landers JP. Nat Protoc. 2015; 10(6): 875–886. [PubMed: 25974096]

Thorslund T, Ripplinger A, Hoffmann S, Wild T, Uckelmann M, Villumsen B, Narita T, Sixma TK, Choudhary C, Bekker-Jensen S. Nature. 2015; 527(7578):389–393. [PubMed: 26503038]

Towner JS, Rollin PE, Bausch DG, Sanchez A, Crary SM, Vincent M, Lee WF, Spiropoulou CF, Ksiazek TG, Lukwiya M. J Virol. 2004; 78(8):4330–4341. [PubMed: 15047846]

Trombley AR, Wachter L, Garrison J, Buckley-Beason VA, Jahrling J, Hensley LE, Schoepp RJ, Norwood DA, Goba A, Fair JN. Am J Trop Med Hyg. 2010; 82(5):954–960. [PubMed: 20439981]

Wang G, Yang F, Zhao W. Lab Chip. 2014; 14(8):1452–1458. [PubMed: 24599543]

Watson D, Russell W, Wildy P. Virology. 1963; 19(3):250–260. [PubMed: 13999204]

Zaki SR, Shieh WJ, Greer PW, Goldsmith CS, Ferebee T, Katshitshi J, Tshioko FK, Bwaka MA, Swanepoel R, Calain P. J Infect Dis. 1999; 179(Supplement 1):36–47.

Zhu X, Vannahme C, Højlund-Nielsen E, Mortensen NA, Kristensen A. Nat Nanotechnol. 2015; 11:325–329. [PubMed: 26657786]

Web References

Solulink: http://www.solulink.com/products/ptm/S-1008-SulfoSFB.pdf (last accessed 10/26/2016)

ZR whole-blood RNA MiniPrep™: https://www.zymoresearch.com/rna/total-rna-purification/blood-body-fluid-rna/zr-whole-blood-rna-miniprep (last accessed 10/26/2016)

Highlights

- An automated microfluidic sample preparation multiplexer (SPM) has been introduced for Ebola virus detection.

- Metered air bubbles injected through pneumatically actuated microvalves are used to enhance the mixing of nucleic acid targets and magnetic beads.

  The total sample preparation and detection time is within two hours. Without target amplification, a significantly improved sensitivity for clinical samples (0.021 pfu/mL) is reported using an on-chip concentration protocol (80X).
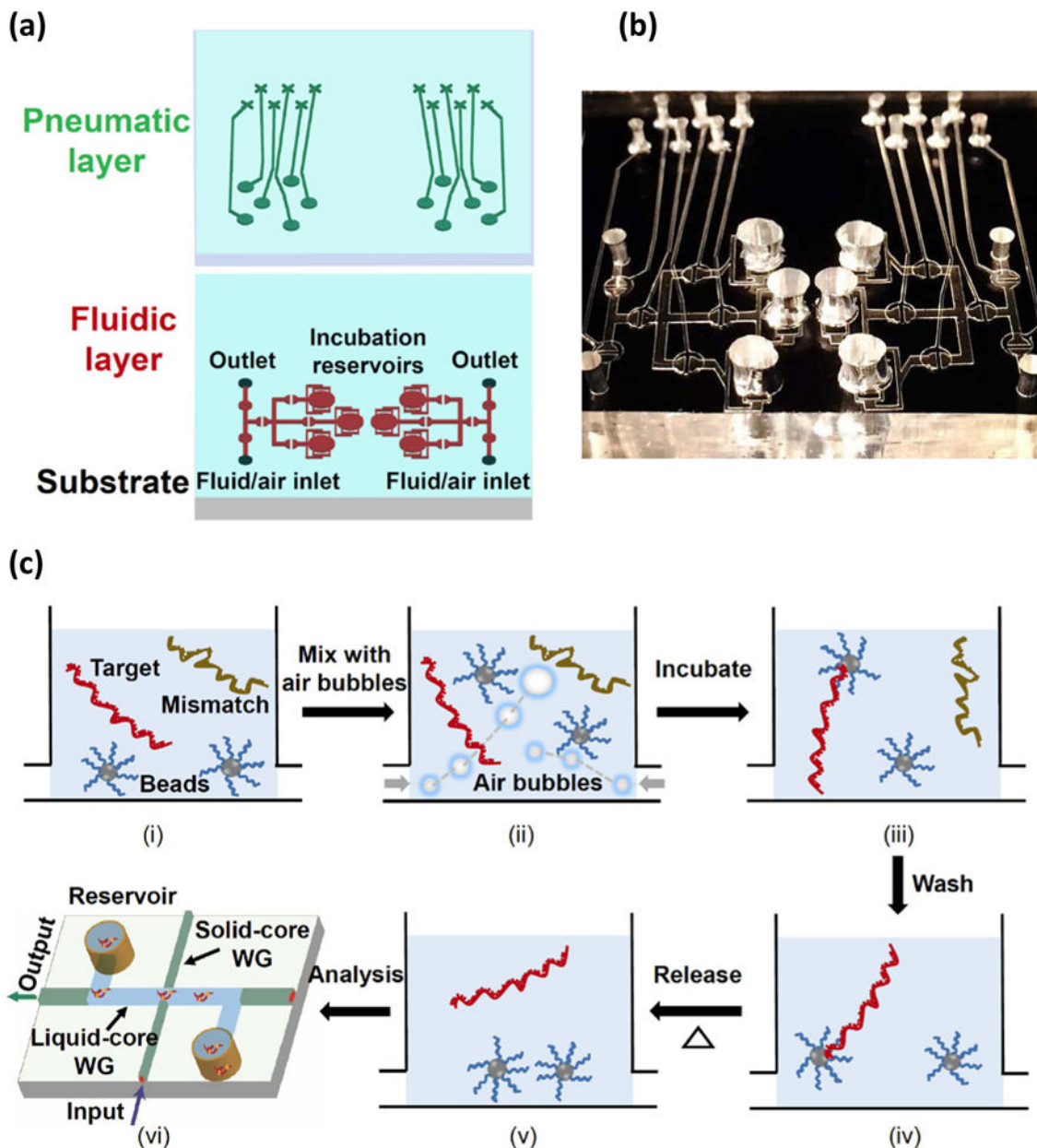
Figure 1.
(a) Design of the sample preparation multiplexer (SPM) with six incubation reservoirs for target preparation. Reagents and metered air bubbles are introduced into the incubation reservoirs by microvalve pumps. (b) Photograph of the SPM. (c) Schematic of the solid-phase extraction process and assay.
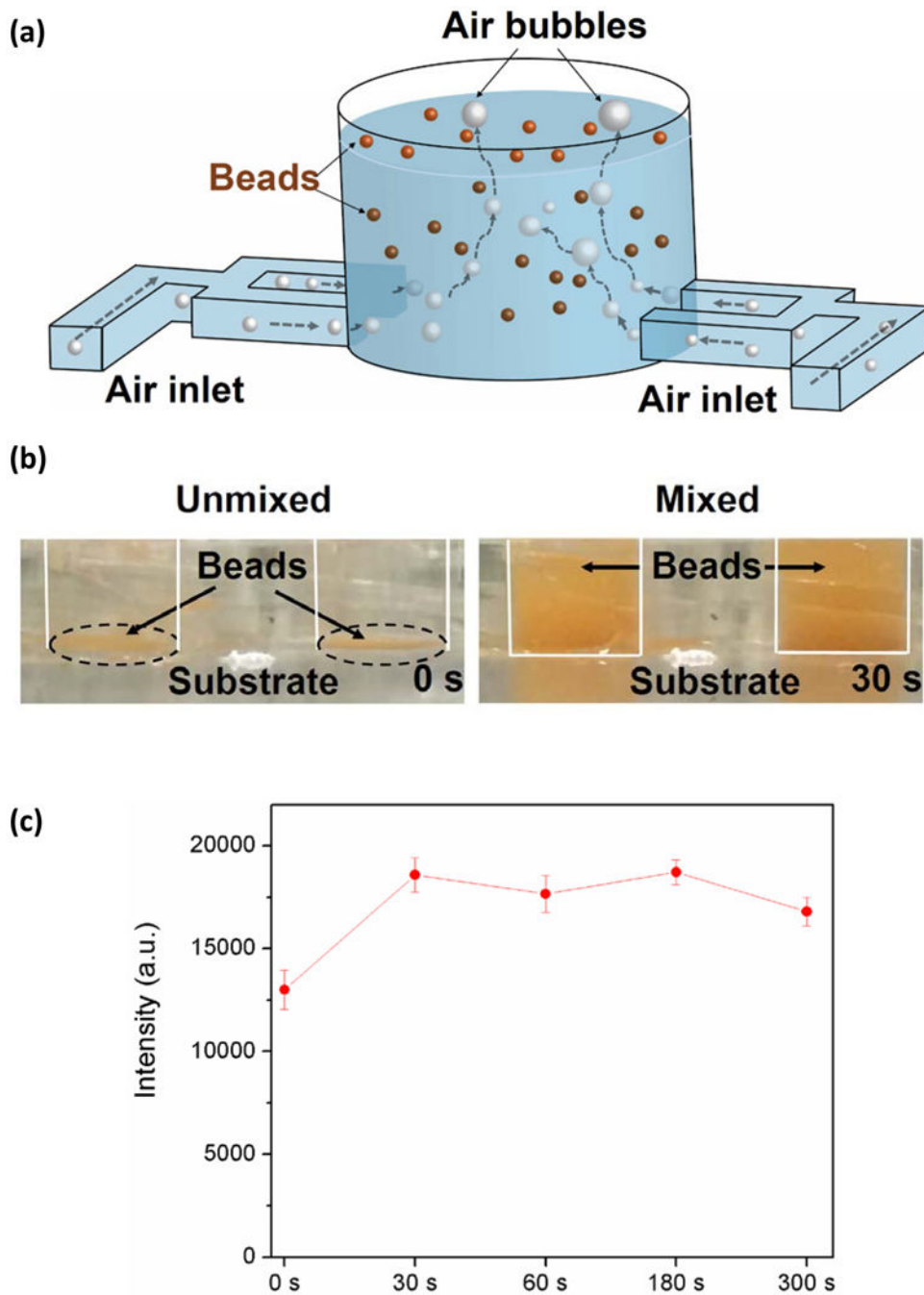
Figure 2.
(a) Schematic of how air bubbles are generated and used to effect mixing in the SPM. (b) Photographs of magnetic bead solution before (0 second) and after (30 seconds) air bubble mixing. A video of mixing is available in the supplement information. (c) Capture efficiency of synthetic nucleic acid target vs. mixing time. Air mixing was applied every 10 minutes during the overall 40 minute incubation time.
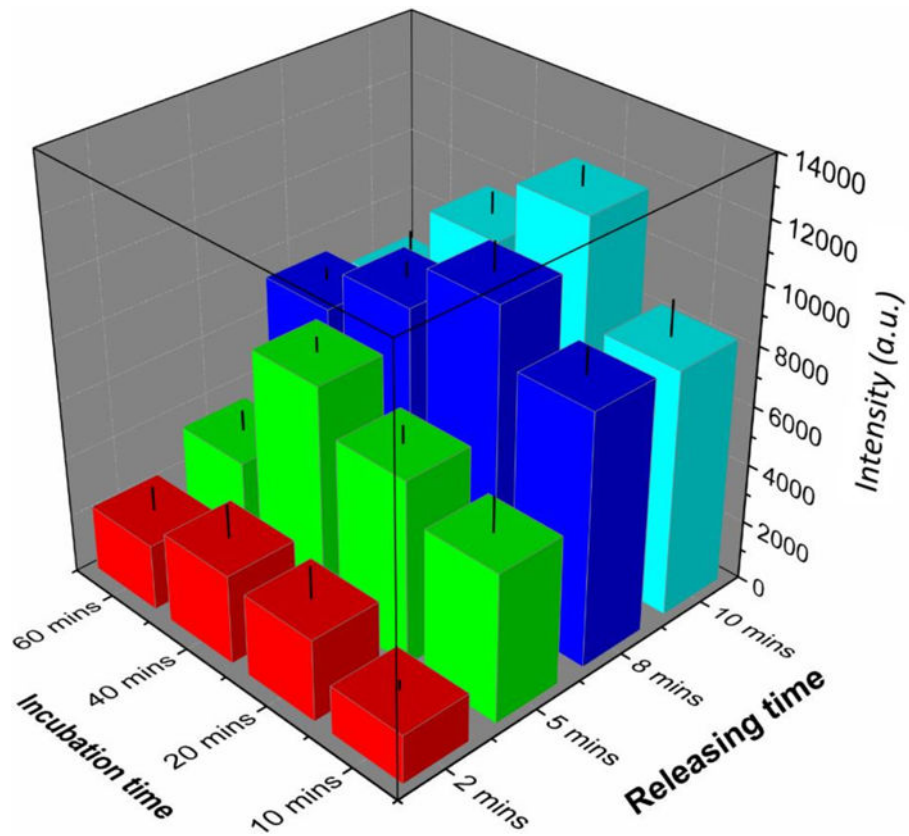
Figure 3.
Optimization of incubation conditions for 100-mer synthetic DNA nucleic acid target capture as a function of incubation time (10 to 60 minutes) and release time (2 to 10 minutes). The release temperature is 80 °C. Thirty seconds of air bubble mixing was applied every 10 minutes during incubation for all samples.
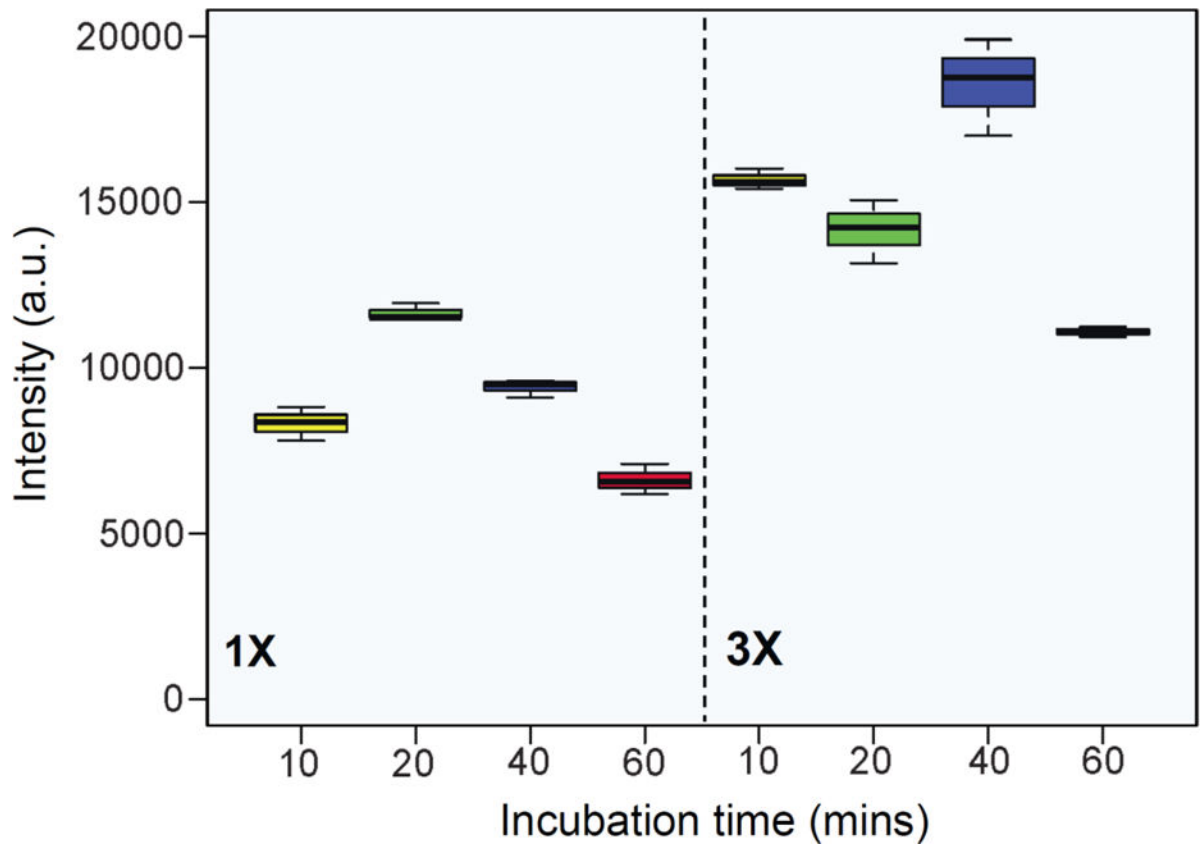
Figure 4.
Capture efficiency results for 1 nM synthetic DNA nucleic acid (1X) as a function of incubation time compared with similar experiments performed with the 3X target concentration procedure. (1X: input 20 μL, release 20 μL; 3X: input 45 μL, release 15 μL)
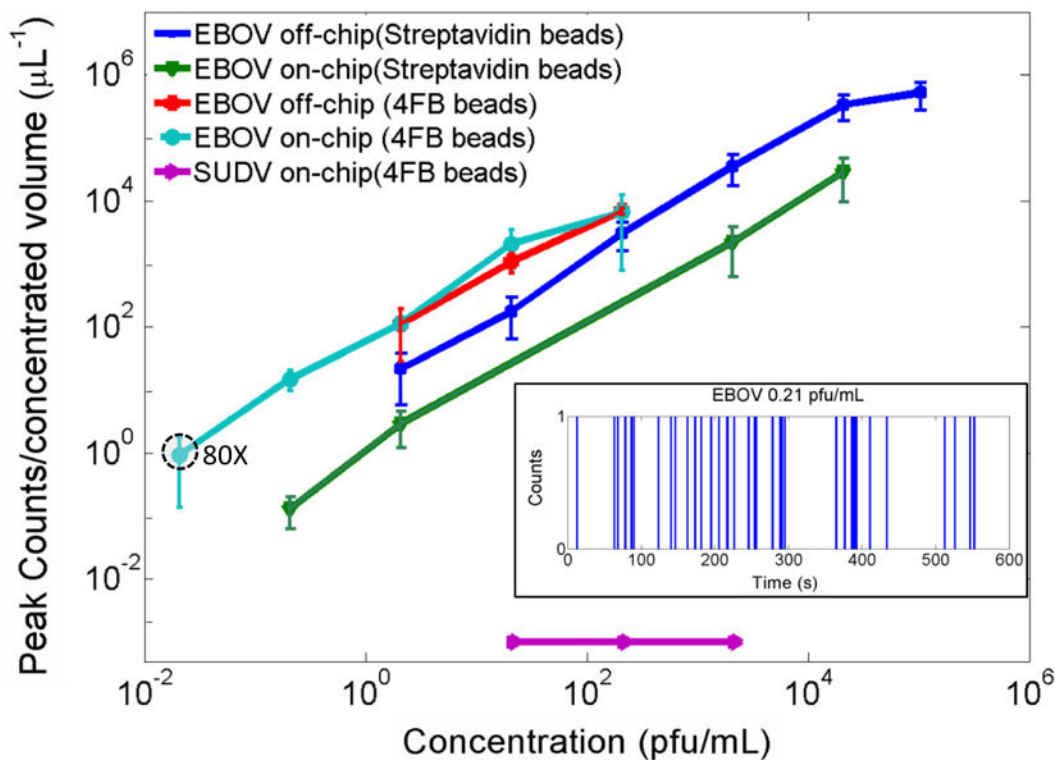
Figure 5.
Detection of Ebola virus with silicon-based optofluidic ARROW chip. Concentration-dependent fluorescence counts for Streptavidin beads (off-chip and on-chip) and 4FB beads (off-chip and on-chip) target capture. No peaks were detected above dye background for negative control samples. (Dark blue and green lines are from reference 12). (Inset) Segments of digitized fluorescence signal above SYBR® Gold dye background indicating single RNA detection events.